ESAIM: PROCEEDINGS, April 2009, Vol. 26, p. 207-216
H. Ammari, Editor

DETECTION OF INTERNAL CORROSION

H. Ammari[1], H. Kang[2] and E. Kim[3]

Abstract. The purpose of this paper is to review recently developed algorithms for corrosion detection and to compare between them.

1. Introduction

Corrosion detection is an important problem in the field of nondestructive evaluation (NDE) for an obvious practical reason, and new techniques are constantly being sought for the detection of hidden corrosion. In relation to the NDE of the corrosion there have been several mathematical works: See, for example, Kaup and Santosa [8], Kaup *et al.* [9], Vogelius and Xu [11], Inglese [7], Luong and Santosa [10], Banks et al. [4] and references therein.

In general corrosion is defect in various phenomena such as electrical defect or defect for the wave propagation or the guided wave. Therefore the methods of detecting corrosion can vary depending on the related physical phenomena. Quite recently various algorithms for corrosion detection are proposed and tested numerically in three different models: the electrostatic model [3], the ultrasound model [2], and the guided wave model [1]. The purpose of this paper is to review the results of these works and compare them.

2. Mathematical models

The electrostatic model of corrosion of this paper is taken from [11], which we review briefly here. Let Ω be a bounded domain in $\mathbb{R}^d$, $d = 2, 3$, and suppose that a corrosion occurs on a part Γ of the boundary $\partial\Omega$ of Ω. Vogelius and Xu derived in [11] that the electrostatic potential u in the presence of corrosion is a solution of the following nonlinear

[1] Institut Langevin, Laboratoire Ondes et Acoustique, CNRS UMR 7587, ESPCI, 10 rue Vauquelin, 75231 Paris Cedex 05, France; email: `habib.ammari@polytechnique.fr`

[2] Department of Mathematics, Inha University, Incheon 402-751, Korea; email: `hbkang@inha.ac.kr`

[3] Ewha Women's University, Seoul 120-750, Korea; email: `kim123ej@hanmail.net`

Article published by EDP Sciences and available at http://www.edpsciences.org/proc
or http://dx.doi.org/10.1051/proc/2009014

boundary value problem:

$$\begin{cases} \Delta u = 0 & \text{in } \Omega, \\ \dfrac{\partial u}{\partial \nu} + \gamma \left(e^{\alpha u} - e^{(\alpha-1)u} \right) = 0 & \text{on } \Gamma, \\ \dfrac{\partial u}{\partial \nu} = g & \text{on } \partial\Omega \setminus \Gamma \end{cases} \tag{2.1}$$

for some constant γ and α, provided that a current flux g is applied on $\partial\Omega \setminus \Gamma$. This nonlinear elliptic equation is derived from the so-called Butler-Volmer formula. By linearizing this nonlinear problem around $u = 0$, the following linear elliptic equation is derived:

$$\begin{cases} \Delta u = 0 & \text{in } \Omega, \\ \dfrac{\partial u}{\partial \nu} + \gamma u = 0 & \text{on } \Gamma, \\ \dfrac{\partial u}{\partial \nu} = 0 & \text{on } \partial\Omega \setminus \Gamma, \end{cases} \tag{2.2}$$

where ν is the outward unit normal to Ω on $\partial\Omega$. Note that the γ in (2.2) is $(2\alpha-1)$ times γ in (2.1). What is important in (2.2) is that the corrosive part of the boundary is characterized by a Robin type boundary condition.

We will be considering a cross section of three dimensional pipeline inside which there are corrosive parts. Thus the specimen Ω to be inspected in this paper is a two dimensional annulus. To be precise, $\Omega = U \setminus \overline{D}$, where U is a simply connected bounded $\mathcal{C}^2$ domain in $\mathbb{R}^2$ and D is a simply connected $\mathcal{C}^2$ domain compactly contained in U. We define $\Gamma_e = \partial U$ and $\Gamma_i = \partial D$ so that $\partial\Omega = \Gamma_i \cup \Gamma_e$, where Γ_e and Γ_i are the external and internal boundaries of Ω, respectively. Suppose that the inaccessible surface Γ_i contains some corrosive parts I_s, $s = 1, \ldots, m$. We assume that the parts I_s are well-separated and the reciprocal of the surface impedance (the corrosion coefficient) of each I_s, $s = 1, \ldots, m$, is $\gamma_s \geq 0$, not identically zero. We also assume that each $\gamma_s \in \mathcal{C}^1(I_s)$. Let

$$\gamma(x) = \sum_{s=1}^{m} \gamma_s \chi_s(x), \quad x \in \Gamma_i, \tag{2.3}$$

where χ_s denotes the characteristic function on I_s. A significant assumption on the corrosion is smallness: We assume that the one-dimensional Hausdorff measures of I_s are small:

$$|I_s| = O(\epsilon), \quad s = 1, \ldots, m, \tag{2.4}$$

where ϵ is a small parameter representing the common order of magnitude of I_s. Here and throughout this paper $|\cdot|$ denotes the one-dimensional Hausdorff measure. It is worth emphasizing that the smallness assumption is on I_s, not on the corrosion coefficient γ_s.

According to (2.2), the voltage potential u_ϵ generated by a voltage f applied on Γ_e satisfies

$$\begin{cases} \Delta u_\epsilon = 0 & \text{in } \Omega, \\ -\dfrac{\partial u_\epsilon}{\partial \nu} + \gamma u_\epsilon = 0 & \text{on } \Gamma_i, \\ u_\epsilon = f & \text{on } \Gamma_e, \end{cases} \tag{2.5}$$

where ν is the outward unit normal to Ω on Γ_e and inward on Γ_i.

Another justification of the mathematical model can be found in the work of Buttazzo and Kohn. The corrosion can be regarded as a thin coating and it is proved in [5] that as the thickness of the coating approaches to zero the boundary condition tends to the Robin boundary condition in (2.5). This justification of the model may be applied to other kinds of corrosion such as the one for the ultrasound wave and the one for the eigen-modes.

The ultrasound wave u_ϵ generated by a source at $y \in \Gamma_e$ in the presence of the corrosion satisfies

$$\begin{cases} (\Delta + \omega^2) u_\epsilon = 0 & \text{in } \Omega, \\ -\dfrac{\partial u_\epsilon}{\partial \nu} + \gamma u_\epsilon = 0 & \text{on } \Gamma_i, \\ u_\epsilon = \Phi_\omega(\cdot - y) & \text{on } \Gamma_e, \end{cases} \tag{2.6}$$

where ω is the frequency of the wave and Φ_ω is the fundamental solution to the Helmholtz equation, *i.e.*,

$$\Phi_\omega(x) = -\frac{i}{4} H_0^{(1)}(\omega |x|), \quad x \neq 0. \tag{2.7}$$

Here $H_0^{(1)}$ is the Hankel function of the first kind of order 0 [6].

On the other hand, the eigenvalue problem in the presence of corrosion consists of finding $\omega_\epsilon > 0$ such that there exists a nontrivial solution v_ϵ to

$$\begin{cases} (\Delta + \omega_\epsilon^2) v_\epsilon = 0 & \text{in } \Omega, \\ -\dfrac{\partial v_\epsilon}{\partial \nu} + \gamma \chi(I) v_\epsilon = 0 & \text{on } \Gamma_i, \\ v_\epsilon = 0 & \text{on } \Gamma_e, \\ \int_\Omega v_\epsilon^2 = 1, \end{cases} \tag{2.8}$$

assuming that there is a single corrosive part I.

The inverse problem considered in the papers [1–3] is to detect the corrosive parts on the inaccessible boundary Γ_i by means of the measurements on the accessible boundary Γ_e. In particular, the aim is to detect the location and the size of the corrosive parts, and the corrosion coefficient γ_s. For the problem (2.5) and (2.6) the measurements are $\frac{\partial u_\epsilon}{\partial \nu}$ on Γ_e, while for the problem (2.8) the measurement is the pair of modal parameters $(\omega_\epsilon, \frac{\partial v_\epsilon}{\partial \nu}|_{\Gamma_e})$. In above mentioned works, various algorithms to detect corrosive parts are proposed and tested numerically. Those algorithms are based on asymptotic expansions of the solutions of the related equations which we review in the next section.

3. Asymptotic expansions

We now review the asymptotic expansions of the measurements as the smallness parameter ϵ tends to zero.

Electrostatic measurements: Let $G(x,z)$ be the Green function for the problem (2.5) with $\gamma = 0$, *i.e.*, for each $z \in \Omega$, $G(x,z)$ is the solution to

$$\begin{cases} \Delta_x G(x,z) = -\delta_z & \text{in } \Omega, \\ \dfrac{\partial}{\partial \nu_x} G(x,z) = 0, & x \in \Gamma_i, \\ G(x,z) = 0, & x \in \Gamma_e. \end{cases} \tag{3.1}$$

Let u_ϵ be the solution to (2.5) and u_0 the one when $\gamma = 0$, *i.e.*, in the absence of the corrosion. Then the following asymptotic expansion holds uniformly for $x \in \Gamma_e$ [3]:

$$\frac{\partial u_\epsilon}{\partial \nu}(x) = \frac{\partial u_0}{\partial \nu}(x) - \sum_{s=1}^{m} \langle \gamma \rangle_s u_0(z_s) \frac{\partial}{\partial \nu_x} G(x, z_s) + O(\epsilon^{1+\alpha}) \tag{3.2}$$

for some $\alpha > 0$, where

$$\langle \gamma \rangle_s := \int_{I_s} \gamma ds,$$

and z_s denotes the location of I_s, $s = 1, \ldots, m$.

Ultrasound measurements: Let G_ω be the Green function for the problem (2.6) with $\gamma = 0$, *i.e.*, for each $z \in \Omega$, $G_\omega(x,z)$ is the solution to

$$\begin{cases} (\Delta_x + \omega^2) G_\omega(x,z) = -\delta_z & \text{in } \Omega, \\ \dfrac{\partial G_\omega}{\partial \nu_x}(x,z) = 0, & x \in \Gamma_i, \\ G_\omega(x,z) = 0, & x \in \Gamma_e. \end{cases} \tag{3.3}$$

Let u_ϵ be the solution to (2.6) and u_0 the one when $\gamma = 0$, *i.e.*, in the absence of the corrosion. Suppose that the wavelength $\lambda = 2\pi/\omega = \epsilon^{1-\beta} (>> \epsilon)$ for some positive constant β, then the following asymptotic formula holds uniformly on Γ_e for some positive constant α [3]:

$$\frac{\partial u_\epsilon}{\partial \nu}(x) = \frac{\partial u_0}{\partial \nu}(x) - \sum_{s=1}^{m} \langle \gamma \rangle_s u_0(z_s) \frac{\partial G_\omega}{\partial \nu}(x, z_s) + O(\epsilon^{1+\alpha}), \quad x \in \Gamma_e. \tag{3.4}$$

Note that (3.2) is at least formally the limiting case ($\omega = 0$) of (3.4).

Modal parameter measurements: Suppose there is a single corrosive part I and the corrosion coefficient γ is constant. Let ω_ϵ and v_ϵ be an eigenvalue of (2.8) and the corresponding (normalized) eigenfunction, respectively, and let ω_0 and v_0 be those in the absence of the corrosion. Then the following asymptotic formula were derived in [1]:

$$\omega_\epsilon = \omega_0 + \frac{\gamma}{2\omega_0} \int_I v_0^2 + O(\epsilon^2) \tag{3.5}$$

as $\epsilon \to 0$. Furthermore,

$$v_\epsilon = v_0 + O(\epsilon) \tag{3.6}$$

where $O(\epsilon)$ is in $H^{3/2}(\Omega)$-norm.

Rigorous derivations of asymptotic expansions can be found in [1–3]. The expansions (3.5) and (3.6) can be seen easily by expanding ω_ϵ and v_ϵ formally as

$$\omega_\epsilon = \omega_0 + \epsilon\omega_1 + \epsilon^2\omega_2 + \dots,$$
$$v_\epsilon = v_0 + \epsilon v_1 + \epsilon^2 v_2 + \dots.$$

4. Corrosion detection algorithms

We now describe three algorithms for detection of internal corrosive parts. They are MUSIC-type algorithms and the vibration test algorithm, and based on the asymptotic expansions explained in the previous section. Since the MUSIC-type algorithms for (2.5) [3] and (2.6) [2] are almost identical, we will only describe the one using the ultrasound measurements.

MUSIC type algorithm. Let, for $z \in \Gamma_i$ and $x \in \Gamma_e$,

$$h_z(x) := \int_{\Gamma_e} \frac{\partial G_\omega}{\partial \nu}(y,z)\Phi_\omega(y-x)\, d\sigma(y).$$

Then the following is the MUSIC characterization of the location of the corrosive parts, a proof of which can be found in [2]:

MUSIC characterization. If there are complex numbers $a_1, \dots, a_m$ such that

$$h_z(y) = \sum_{s=1}^{m} a_s h_{z_s}(y) \quad \text{for all } y \in \Gamma_e, \tag{4.1}$$

then $z \in \{z_1, \dots, z_m\}$.

Let us now discretize the relation (4.1) with sampling points $\{y_1, \dots, y_N\}$ on Γ_e. Let

$$v_s = \Big(h_{z_s}(y_1), \dots, h_{z_s}(y_N)\Big)^T, \quad s = 1, \dots, m, \tag{4.2}$$

where T denotes the transpose. Then the discrete version of (4.1) is

$$\Big(h_z(y_1), \dots, h_z(y_N)\Big)^T \quad \text{is a linear combination of } \{v_1, \dots, v_m\}. \tag{4.3}$$

So the question now is how to characterize those points z such that (4.3) holds. It should be emphasized that the values $h_{z_s}(y_j)$ are not known since the location of corrosive parts z_s is not known. But we claim that (4.3) can be checked using the boundary measurements and the asymptotic formula (3.4) plays a central role in this, as we see in the following.

Let us first introduce the notion of the Dirichlet-to-Neumann (DtN) map. Let u be the solution to the problem

$$\begin{cases} (\Delta + \omega^2)u = 0 & \text{in } \Omega, \\ -\dfrac{\partial u}{\partial \nu} + \gamma u = 0 & \text{on } \Gamma_i, \\ u = f & \text{on } \Gamma_e, \end{cases}$$

and define the DtN map Λ_γ^ω by

$$\Lambda_\gamma^\omega(f) := \frac{\partial u}{\partial \nu}\Big|_{\Gamma_e}. \tag{4.4}$$

Let Λ_0^ω be the DtN map when there is no corrosion.

By the definition of the Green function G_ω, we have $h_z(x) = -u_0(z)$ where u_0 is the solution to

$$\begin{cases} (\Delta + \omega^2)u_0 = 0 & \text{in } \Omega, \\ \dfrac{\partial u_0}{\partial \nu} = 0 & \text{on } \Gamma_i, \\ u_0 = \Phi_\omega(\cdot - x) & \text{on } \Gamma_e. \end{cases}$$

Thus it follows from (3.4) that

$$(\Lambda_\gamma^\omega - \Lambda_0^\omega)(\Phi_\omega(\cdot - x))(y) \approx \sum_{s=1}^m \langle\gamma\rangle_s h_{z_s}(x) \frac{\partial G_\omega}{\partial \nu}(y, z_s), \quad x, y \in \Gamma_e. \tag{4.5}$$

By integrating both sides of the above relation against $\Phi_\omega(\cdot - t)$ for $t \in \Gamma_e$, we obtain

$$\int_{\Gamma_e} (\Lambda_\gamma^\omega - \Lambda_0^\omega)(\Phi_\omega(\cdot - x))(y)\Phi_\omega(y - t)\, d\sigma(y) \approx \sum_{s=1}^m \langle\gamma\rangle_s h_{z_s}(x) h_{z_s}(t), \quad x, t \in \Gamma_e.$$

In particular, we have

$$\int_{\Gamma_e} (\Lambda_\gamma^\omega - \Lambda_0^\omega)(\Phi_\omega(\cdot - y_i))(y)\Phi_\omega(y - y_j)\, d\sigma(y) \approx \sum_{s=1}^m \langle\gamma\rangle_s h_{z_s}(y_i) h_{z_s}(y_j), \quad i, j = 1, \ldots, N. \tag{4.6}$$

Let $A := (a_{ij})$ where

$$a_{ij} := \sum_{s=1}^m \langle\gamma\rangle_s h_{z_s}(y_i) h_{z_s}(y_j), \quad i, j = 1, \ldots, N.$$

One can easily see that (4.3) is equivalent to

$$h_z := \Big(h_z(y_1), \ldots, h_z(y_N)\Big)^T \in \text{Range}(A). \tag{4.7}$$

Let

$$A^c := \left(\int_{\Gamma_e} (\Lambda_\gamma^\omega - \Lambda_0^\omega)(\Phi_\omega(\cdot - y_i))(y)\Phi_\omega(y - y_j)\, d\sigma(y) \right)_{i,j=1,\ldots,N}. \tag{4.8}$$

Note that A^c can be computed from the boundary measurements $(\Lambda_\gamma^\omega - \Lambda_0^\omega)(\Phi_\omega(\cdot - y_i))$. The relation (4.6) shows that A^c gives an approximation of A. Since A and A^c are symmetric matrices, they admit (orthogonal) singular value decompositions (SVD). The number of significant eigenvalues of A is exactly the number of corrosive parts. But we do not have A as our data. Instead we have A^c which is only approximation of A. Moreover, the SVD of A^c does not exhibit a clear drop of the eigenvalues as one can see from Figure 1. It means that we can not determine the number of corrosive parts from the SVD of A^c.

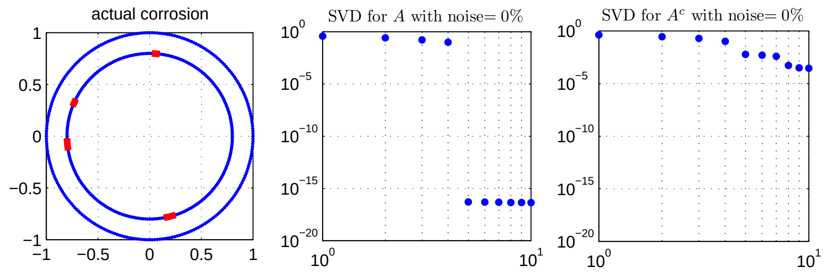

FIGURE 1. SVD of A and A^c.

In order to overcome this difficulty we proceed as follows: Let

$$A^c = \sum_{n=1}^{N} \lambda_n v_n \otimes v_n$$

be the SVD of A^c where $\lambda_1 \geq \lambda_2 \geq \ldots \geq \lambda_N$ are eigenvalues of A^c and v_n are corresponding eigenvectors. For $k = 1, 2, \ldots, N$, let S_k be the space spanned by $v_1, \ldots, v_k$, and let P_k be the orthogonal projector from $\mathbb{R}^N$ onto S_k. Define $\theta_k(z)$ by

$$\cot \theta_k(z) = \frac{\|P_k^\epsilon(h_z)\|}{\|(I - P_k^\epsilon)(h_z)\|}, \quad z \in \Gamma_i,$$

and compute the minimal value of θ_k. We repeat this process for $k = 1, 2, \ldots$ until the minimal values are stabilized. It turned out that this MUSIC type algorithm detect the number of corrosive parts m and their locations z_s pretty well. See [2, 3]. We will present some computational results in the next section.

Once the locations of the corrosive parts were found, it is straightforward to compute the (averaged) corrosion coefficients $\langle\gamma\rangle_s$ using (3.2) and (3.4). We omit this.

We note that the same algorithm works for the electrostatic measurement problem (2.5). It is worth emphasizing that the algorithm is a direct *not* iterative one in the sense that the computation at each step does not use the results of the previous steps.

Vibration test algorithm. We now review the algorithm for the vibration test which is based on the asymptotic expansion (3.5) and (3.6). This algorithm was proposed and tested numerically in [1].

For h such that $\int_{\Gamma_e} h \frac{\partial v_0}{\partial \nu} = 0$, let $w_h \in H^1(\Omega)$ be the solution to

$$\begin{cases} (\Delta + \omega_0^2) w_h = 0 & \text{in } \Omega, \\ \dfrac{\partial w_h}{\partial \nu} = 0 & \text{on } \Gamma_i, \\ w_h = h & \text{on } \Gamma_e. \end{cases} \tag{4.9}$$

Applying Green's formula, we obtain

$$\gamma \int_I w_h v_\epsilon = \int_{\Gamma_i} w_h \frac{\partial v_\epsilon}{\partial \nu} = \int_{\Gamma_e} h \frac{\partial v_\epsilon}{\partial \nu} + (\omega_\epsilon^2 - \omega_0^2) \int_\Omega v_\epsilon w_h. \tag{4.10}$$

Dividing (4.10) by $\omega_\epsilon^2 - \omega_0^2$ and using (3.5) we induce

$$\frac{\displaystyle\int_I w_h v_\epsilon}{\displaystyle\int_I v_0^2} = \frac{1}{\omega_\epsilon^2 - \omega_0^2} \int_{\Gamma_e} h \frac{\partial v_\epsilon}{\partial \nu} + \int_\Omega v_\epsilon w_h + O(\epsilon). \tag{4.11}$$

By (3.6), we have

$$\int_I w_h v_\epsilon = \int_I w_h v_0 + O(\epsilon^2),$$
$$\int_\Omega v_\epsilon w_h = \int_\Omega v_0 w_h + O(\epsilon).$$

Therefore, we have

$$\frac{w_h(z)}{v_0(z)} - \int_\Omega v_0 w_h \approx \frac{1}{2\omega_0(\omega_\epsilon - \omega_0)} \int_{\Gamma_e} \frac{\partial v_\epsilon}{\partial \nu} h. \tag{4.12}$$

This is the key observation on which our reconstruction procedure is based. Since we are in possession of $\omega_\epsilon - \omega_0$ and $\frac{\partial v_\epsilon}{\partial \nu}|_{\Gamma_e}$ by the boundary measurements, the reconstruction algorithm is as follows. Let $h = h_1, h_2, \ldots, h_n$, where $\{h_i\}_{i=1}^n$ is a set of n independent functions satisfying $\int_{\Gamma_e} h_i \frac{\partial v_0}{\partial \nu} = 0$ for $i = 1, \ldots, n$. For any $y \in \Gamma_i$ such that $v_0(y) \neq 0$ compute $(w_{h_i}/v_0)(y)$ and $\int_\Omega v_0 w_h$. The point z can be found as the minimum point of

$$J(z) := \sum_{i=1}^n \left| \frac{w_{h_i}(z)}{v_0(z)} - \int_\Omega v_0 w_{h_i} - \frac{1}{2\omega_0(\omega_\epsilon - \omega_0)} \int_{\Gamma_e} \frac{\partial v_\epsilon}{\partial \nu} h_i \right|. \tag{4.13}$$

5. Numerical examples

This section presents numerical results of finding the internal corrosive parts by electrostatic, ultrasound, and vibration tests explained in the previous sections, for the purpose of comparing their performance. In the following, $\Omega \subset \mathbb{R}^2$ is assumed to be the annulus centered at $(0,0)$ with radii, r_e and r_i. Let $I_s, s = 1, \cdots, m$, be the corrosive parts with the corrosive coefficients, γ_s. Let z_s and $\langle\gamma\rangle_s$ be the center and the integration of corrosive part I_s, and z_s^c and $\langle\gamma\rangle_s^c$ the detected ones.

For computation, we discretize Γ_e and Γ_i by

$$\Gamma_e = \{r_e(\cos\theta_n, \sin\theta_n) | \theta_n = 2\pi(n-1)/N, n = 1, \cdots, N\}$$

and

$$\Gamma_i = \{r_i(\cos\theta_n, \sin\theta_n) | \theta_n = 2\pi(n-1)/N, n = 1, \cdots, N\}$$

with $N = 256$. In the following example, the outer radius $r_e = 1$ and the inner one $r_i = 0.8$. We do process under noise= $0\%, 1\%, 5\%$ and 10%. Here $p\%$ noise means that we add $p\%$

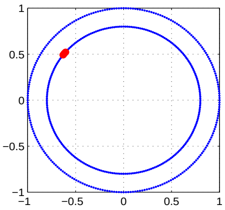

Actual data

γ_1	z_1	$\langle\gamma\rangle_1$	$\|I_1\|$
1	(-0.6184, 0.5075)	0.0589	0.0589

Detected data

	Electrostatic M.		Ultrasound M.		Modal Parameter M.	
noise(%)	$\|z_1 - z_1^c\|$	$\|\langle\gamma\rangle_1 - \langle\gamma\rangle_1^c\|$	$\|z_1 - z_1^c\|$	$\|\langle\gamma\rangle_1 - \langle\gamma\rangle_1^c\|$	$\|z_1 - z_1^c\|$	$\|\langle\gamma\rangle_1 - \langle\gamma\rangle_1^c\|$
0	0.0000	4.8253e-4	0.0000	3.7965e-3	0.0196	1.4267e-2
1	0.0000	4.7000e-4	0.0000	3.7979e-3	0.0393	1.3352e-2
5	0.0000	4.1966e-4	0.0000	3.7989e-3	0.0393	9.3961e-3
10	0.0000	3.5622e-4	0.0000	3.8013e-3	0.0785	1.7248e-2

FIGURE 2. The computational results in the case of a single corrosive part.

random noise of the L^2-norm of the the measured data w on Γ_e. Thus, when it comes to the electrostatic and ultrasound measurements, the data with $p\%$ noise is the $N \times N$ matrix

$$(\Lambda_\gamma - \Lambda_0)(\frac{\partial G}{\partial \nu}) + \frac{p}{100} rand(1) \frac{\|(\Lambda_\gamma - \Lambda_0)(\frac{\partial G}{\partial \nu})\|_{L^2(\Gamma_e \times \Gamma_i)}}{\|1\|_{L^2(\Gamma_e \times \Gamma_i)}},$$

and

$$(\Lambda_\gamma - \Lambda_0)(\Phi_\omega) + \frac{p}{100} rand(1) \frac{\|(\Lambda_\gamma - \Lambda_0)(\Phi_\omega)\|_{L^2(\Gamma_e \times \Gamma_i)}}{\|1\|_{L^2(\Gamma_e \times \Gamma_i)}},$$

where $rand(1)$ is the random number in $(-1, 1)$. When we consider the modal parameter measurement, we add $p\%$ noise to the eigenvectors, v_0 and v_ϵ.

Example 1. In this example, we compare the numerical results of three different methods when there is a single corrosive part I_1. We take $\omega = 5$ in the case of ultrasound measurements. Figure 2 summarizes the actual and computational results with noise= $0\%, 1\%, 5\%, 10\%$, respectively. The results show that the MUSIC algorithms using electrostatic and ultrasound measurements detect the location pretty well. Even if the performance of the vibration test is still satisfactory, it is worst among three method. This is natural in a sense that the vibration test uses a single measurement of modal parameters while the other two use multiple measurements.

Example 2. In this example, we consider the case where there are three corrosive parts. Since the vibration test is difficult to apply to the case with multiple corrosive parts, we use only the electrostatic and ultrasound measurements, and compare the computational results. The actual data is summarized in the top of Figure 3. The table shows the computational results under noise= $0\%, 1\%, 5\%, 10\%$. It is interesting to find that those corrosive parts which are close to each other are detected as a single one as the noise level increases.

H.A. is partially supported by the Brain Pool Korea Program at Seoul National University, H.K. is partially supported by the grant KOSEF R01-2006-000-10002-0, and E.K. is supported by BK21 Math. division at Seoul National University.

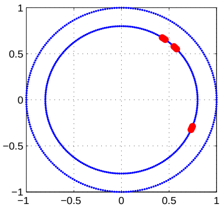

Actual data

m	ω	γ_k	z_k	$\langle\gamma\rangle_k$	$\lvert I_k\rvert$
3	1	0.1	(0.5372, 0.5928)	0.0059	0.0589
		0.05	(0.4445, 0.6652)	0.0029	0.0589
		1	(0.7391,-0.3061)	0.0589	0.0589

Detected data

	Electrostatic M.			Ultrasound M.		
noise(%)	m^c	$\lvert z_k - z_k^c\rvert$	$\lvert\langle\gamma\rangle_k - \langle\gamma\rangle_k^c\rvert$	m^c	$\lvert z_k - z_k^c\rvert$	$\lvert\langle\gamma\rangle_k - \langle\gamma\rangle_k^c\rvert$
0	3	0.0000	4.4419e-5	2	0.0393	2.8423e-3
		0.0000	1.5578e-5			
		0.0000	4.8254e-4		0.0000	3.0922e-3
1	3	0.0000	3.4664e-5	2	0.0196	2.8608e-3
		0.0000	2.7453e-6			
		0.0000	4.7460e-4		0.0000	3.1920e-3
5	2	0.0000	2.3172e-3	2	0.0393	2.8293e-3
		0.0000	4.4258e-4		0.0000	3.0990e-3
10	2	0.0196	2.2691e-3	2	0.0393	2.8163e-3
		0.0000	4.0228e-4		0.0000	3.1058e-3

FIGURE 3. The computational results in the case of multiple corrosive parts.

REFERENCES

[1] H. Ammari, H. Kang, E. Kim, H. Lee, and K. Louati, Vibration testing for detecting internal corrosion, Stud. Appl. Math. 122(1) (2009), 85-104.
[2] H. Ammari, H. Kang, E. Kim, M. Lim, and K. Louati, Ultrasound imaging of internal defects, in preparation.
[3] H. Ammari, H. Kang, E. Kim, K. Louati, and M. Vogelius, A MUSIC-type algorithm for detecting internal corrosion from electrostatic boundary measurements, Numer. Math., 108 (2008), 501-528.
[4] H.T. Banks, M.L. Joyner, B. Wincheski, and W.P. Winfree, Real time computational algorithms for eddy-current-based damage detection, Inverse Problems, 18 (2002), 795-823.
[5] G. Buttazzo and R.V. Kohn, Reinforcement by a thin layer with oscillating thickness, Appl. Math. Opt., 16 (1988), 247-261.
[6] D. Colton and R. Kress, *Inverse Acoustic and Electromagnetic Scattering Theory*, 2nd ed. Berlin, Germany: Springer-Verlag, 1998.
[7] G. Inglese, An inverse problem in corrosion detection, Inverse Problems, 13 (1997), 977-994.
[8] P. Kaup and F. Santosa, Nondestructive evaluation of corrosion damage using electrostatic measurements, J. Nondestructive Eval. 14 (1995), 127-136.
[9] P. Kaup, F. Santosa, and M. Vogelius, A method for imaging corrosion damage in thin plates from electrostatic data, Inverse Problems, 12 (1996), 279-293.
[10] B. Luong and F. Santosa, Quantitative imaging of corrosion inplates by eddy current methods, SIAM J. Appl. Math., 58 (1998), 1509-1531.
[11] M. Vogelius and J. Xu, A nonlinear elliptic boundary value problem related to corrosion modelling, Quart. Appl. Math., 56 (1998), 479-505.